Iranian Polymer Journal (2023) 32:1307–1319
https://doi.org/10.1007/s13726-023-01206-4

ORIGINAL RESEARCH

Self-healable polymer networks from bio-based platform chemicals through Passerini and Diels–Alder reactions: a preliminary study

Qinsheng Li[1] · Yupeng Li[1] · Yaru Li[1] · Qinghua Huang[1] · Zhongyu Hu[1] · Yuping Yang[1] · Zhenhua Xiong[1] · Chuanjie Cheng[1]

Received: 8 February 2023 / Accepted: 13 June 2023 / Published online: 21 July 2023

Abstract

It is urgent and important to design and prepare functional polymers utilizing biomass or bio-based platform chemicals due to fossil resource/energy crisis. We designed and synthesized two linear polymers $\mathbf{LP_1}$ and $\mathbf{LP_2}$ from bio-based platform chemical furfural as well as other biomass-derived feedstock adipic acid and 1,6-hexadiamine using efficient and 100% atom-economy Passerini three-component reaction. The number-average molecular weights of $\mathbf{LP_1}$ and $\mathbf{LP_2}$ are 2189 da and 5464 da, respectively. The products $\mathbf{LP_1}$ and $\mathbf{LP_2}$ were crosslinked with *N,N´*-4,4´-diphenylmethyene bismaleimide (BMI) through Diels–Alder cycloaddition reactions to form the corresponding polymer networks $\mathbf{CP_1}$ and $\mathbf{CP_2}$, respectively. Both $\mathbf{CP_1}$ and $\mathbf{CP_2}$ showed good chemical resistance to acid and ethyl acetate, but relatively poor resistance toward base and THF. Gel fraction values of $\mathbf{CP_1}$ and $\mathbf{CP_2}$ were 82% and 74%, respectively, indicating that most of the linear segments of $\mathbf{LP_1}$ and/or $\mathbf{LP_2}$ were crosslinked after Diels–Alder reactions. Thermal property analysis indicated that the two polymer networks were at rubbery state as their T_g values were 14.78 and 7.00 °C, respectively. Td_{10} values of $\mathbf{CP_1}$ and $\mathbf{CP_2}$ were 151 °C and 131 °C, respectively. The presence of dynamic D–A bonds caused both $\mathbf{CP_1}$ and $\mathbf{CP_2}$ to exhibit intrinsic self-healable performance at 60 °C or higher. Furthermore, $\mathbf{CP_2}$ also showed rapid self-healing behavior (within 3 min) under UV (360 nm) irradiation due to the existence of dynamic disulfide bonds in the main chain.

✉ Chuanjie Cheng
chengcj530@163.com

[1] School of Chemistry and Chemical Engineering, Jiangxi Science & Technology Normal University, Fenglin Street, Nanchang 330013, Jiangxi, People's Republic of China

Graphical abstract

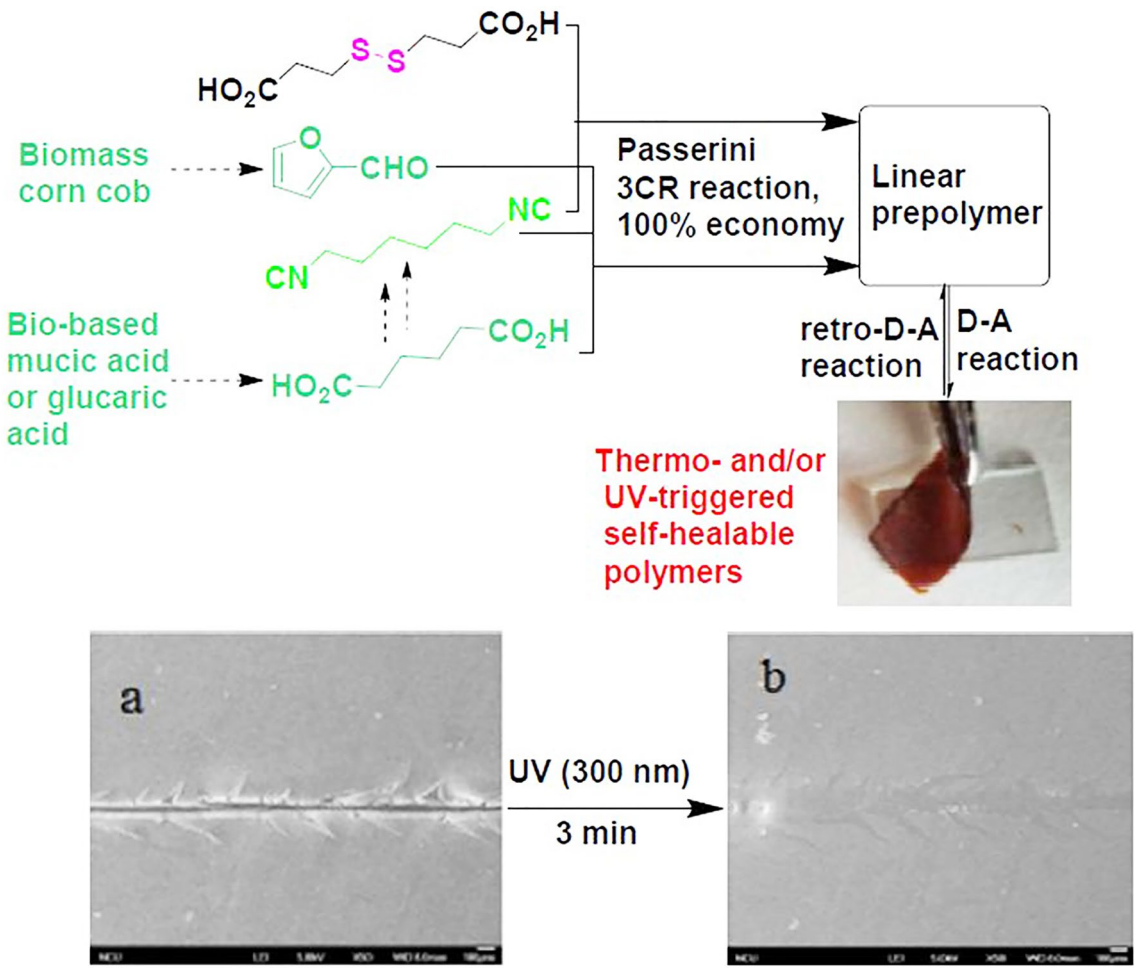

Keywords Self-healable polymers · Passerini reaction · Furfural · Platform chemicals · Diels–Alder reaction

Introduction

Fossil resource crisis motivates world scientists to explore other substitutes. Renewable resources from plants and animals are inexhaustible to some extent due to their possible involvement in ecological system [1–3]. In fact, some common renewable resources, such as cellulose and lignin, have been extensively studied and applied in recent decades [4, 5]. Among various bio-mass resources, furfural and its derivatives can be readily produced from agricultural feedstock, such as wheat bran, corncobs, and sawdust [6, 7]. A variety of useful organic chemicals and polymers have been prepared from furfural and its derivatives [8–10]. For example, Zhang's research group reported synthesis of bis(hydroxylmethylfurfuryl) amines (BHMFAs) from 5-hydroxymethylfurfural (5-HMF) through reductive amination using Ru(II) catalysts, thus avoiding use of cost and toxic $Na(CN)BH_3$ reductant [11]. BHMFAs are expected to be a new group of inspiring furan-based monomers that can be used to synthesize biopolymers, such as polyesters and polyurethanes. More recently, renewable polyurethanes were provided by Kieber III and coworkers by utilizing isohexides and 5-hydroxymethylfurfural [12].

Exploration and application of atom-economic and highly efficient reactions are always the goals of chemists [13]. Multi-component reaction (MCR) is a powerful tool to meet the requirements of this object due to its feature of high efficiency, atom-economy, molecular diversity, cheap reactants, etc. [14–16]. MCRs were previously applied to synthesize small organic molecules [17–19], yet, preparation of polymers through this methodology has also attracted extensive attention in recent years [20–22]. Passerini three-component reaction (Passerini 3-CR) and Ugi four-component reaction (Ugi 4-CR) are undoubtedly two of the most investigated

MCRs both in small molecular and macromolecular syntheses [23–25]. The popular application of these two MCRs lies in that α-acetoxyamides and α-acetamidoamides with multifunctional groups can be formed in one step without using any catalyst. For instance, a pioneering work reported by Zhang and coworkers indicated that polypeptoids can be prepared from natural amino acids by Ugi reaction [26]. Using their method, structurally diverse and functional biocompatible polypeptoids, including γ- and δ-, and poly(ε-peptoid)s, may be obtained under mild conditions (e.g., room temperature, open to air, and catalyst free). Another interesting work is an efficient preparation of redox-responsive poly(ester-amide)s that contain phenylboronic acid esters by Passerini MCR by Li and Du's research group, meaning that these polymers have potential application as H_2O_2-responsive delivery vehicles [27].

Smart polymers are special functional materials which can respond to environmental or factitious stimuli, such as light, heating, redox, pH, and magnetic and mechanical forces [28–30]. Response of smart materials may be changes of volume or shape, sol–gel transformation, solid–liquid conversion, reversible or irreversible cleavage and coupling, hydrophobic-hydrophilic transitions, etc. In recent years, stimulus-responsive self-healing polymers have drawn much attention for their interesting properties and potential applications in electronic devices, soft materials, biomimetic materials, composite materials, etc.[31–33].

Taking all the antecedents into consideration, the aim of present work was to synthesize novel linear polymers from bio-based furfural and other renewable stocks through Passerini three-component reaction, followed by subsequent Diels–Alder crosslinking reaction to prepare thermosets with covalent adaptable networks. The functional polymers showed thermal and/or UV-triggered self-healable properties. Our work features renewable stocks, atom-economic reaction and functional polymers.

Experimental

Materials

1,6-Diaminohexane, diisopropyl amine, phosphorous oxychloride, *N,N´*-4,4´-diphenylmethyene bismaleimide (BMI), furfural, adipic acid, 3,3´-dithiodipropionic acid, ethyl format, 1,4-dioxane, methanol, ethyl acetate, petroleum ether (60–90), dichloromethane (DCM), tetrahydrofuran (THF), toluene, ethanol, and NaOH were purchased from Shanghai Aladdin Biochemical Technology Co. Ltd, China and were used straightly without any purification. Silica gel for column chromatography was obtained from Qingdao Haiyang Chemical Co. Ltd, China.

Characterization

Gel permeation chromatography (GPC) was conducted on an HP 1100 HPLC (America), equipped with a Waters 2414 refractive index detector and three Styragel HR 2, HR 4, HR 5 of 300 × 7.5 mm columns (packed with 5 mm particles of different pore sizes). The column packing allowed the separation of polymers over a wide molecular weight range of 500–1,000,000. THF was used as the eluent at a flow rate of 1 mL/min at 40 °C. PMMA standards were used as the reference. Structures of monomers and linear polymers were characterized by ^{1}H NMR spectroscopy on a Bruker AV 400 MHz spectrometer (Germany). $CDCl_3$ was used as the solvent. The FTIR spectra were recorded through the KBr pellet method using a Bruker V70 FTIR spectrophotometer (Germany). Glass transition temperature (T_g) of polymers was determined by a DSC-204F1 differential scanning calorimeter produced by German NETZSCH corporation. Temperature rising rate was 10 °C/min under N_2 atmosphere. Thermogravimetric analysis (TGA) was measured by NETZSCH TG 209F3, Germany.

Synthesis of 1,6-diisocyanohexane (1)

This compound was synthesized according to the method reported by Gulevich and coworkers [34]. To a 50 mL three-necked flask were added ethyl formate (17.20 mL, 200 mmol) and 1,6-diaminohexane (1.00 g, 8.61 mmol) to form a solution, which was then refluxed overnight. After cooling to room temperature, the mixture was evacuated at room temperature to remove liquor under reduced pressure, followed by adding DCM (17.5 mL) and diisopropyl amine (8.71 g, 86.1 mmol). Phosphorous oxychloride (3.69 g, 24.1 mmol) was added dropwise to the reaction mixture and cooled by an ice bath. After adding phosphorous oxychloride, the reaction system was stirred for 1 h in the ice bath. Then the ice bath was removed and stirring was continued for 6 h. The mixture was poured into 50 mL of K_2CO_3 (10.0 g) aqueous solution. The organic layer was separated, and the aqueous phase was extracted with DCM for three times, and the combined organic phase was dried with anhydrous K_2CO_3 followed by removing DCM to obtain brown oil as a crude product. The oil was purified on a silica gel column with petroleum ether/ethyl acetate (2:1 v:v) as eluent to achieve light yellow oil (0.89 g, 76%). ^{1}H NMR (400 MHz, $CDCl_3$, δ ppm): 3.43–3.37 (m, 4H), 1.75–1.65 (m, 4H), 1.55–1.45 (m, 4H).

Synthesis of linear polymer LP_1 through Passerini reaction

The polymer $\mathbf{LP_1}$ was prepared by modification of the method from Li's research group [35]. Furfural (192 mg,

2 mmol), 1,6-diisocyanohexane (**1**) (136 mg, 1 mmol), adipic acid (146 mg, 1 mmol), and DCM (5 mL) were added to a 50 mL flask. The mixture was stirred at 30 °C for 36 h under N_2 protection. Viscous liquid was obtained after distilling off the solvent DCM. The crude viscous liquid was again dissolved in 1 mL of DCM, and 10 mL petroleum ether was added to precipitate brown oligomer $\mathbf{LP_1}$ (219 mg, 46.2%). M_n 2189 g/mol (measured by GPC). ^{1}H NMR (400 MHz,$CDCl_3$, δ ppm): 7.42–7.39 (s, 2H), 6.52–6.41 (s, 2H), 6.40–6.35 (s, 2H), 6.23–6.17 (s, 2H), 3.23–3.35 (m, 5H), 2.97–2.87 (m, 5H), 2.52–2.40 (m, 4H), 1.37–1.30 (m, 5H). IR (KBr) ν, 3340, 3081, 2931, 2852, 1754, 1530, 1126 cm^{-1}.

Synthesis of crosslinked polymer CP_1 through D–A reaction

The polymer $\mathbf{CP_1}$ was prepared according to the method of our previous work [36]. The linear oligomer $\mathbf{LP_1}$ (474 mg), *N,N´*-4,4´-diphenylmethyene bismaleimide (BMI) (360 mg) and 1,4-dioxane (5 mL) were sequentially added to a 25 mL flask, and the mixture was stirred at 78 °C for 10 h under N_2 atmosphere. Then part of the mixture was coated on a glass substrate to form a film. The left part was continued stirring at 78 °C for another 38 h to obtain brown gel-like polymer $\mathbf{CP_1}$ (530 mg, c.a. 64%). The glass transition temperature (T_g) of $\mathbf{CP_1}$ was 14.78 °C. IR (KBr) ν: 2931, 2845, 1773, 1692, 1407 cm^{-1}.

Synthesis of linear polymer LP_2 through Passerini reaction

The polymer $\mathbf{LP_2}$ was synthesized by the method similar to that of $\mathbf{LP_1}$ [35]. Furfural (192 mg, 2 mmol), 1,6-diisocyanohexane (**1**) (136 mg, 1 mmol), 3,3'-dithiodipropionic acid (210 mg, 1 mmol), and DCM (5 mL) were added to a 50 mL flask. The mixture was stirred at 30 °C for 36 h under nitrogen protection in a dark place. Viscous liquid was obtained after distilling off the solvent DCM. The crude viscous liquid was again dissolved in 1 mL of DCM, and 10 mL petroleum ether was added to precipitate brown oligomer $\mathbf{LP_2}$ (299 mg, 55.6%). M_n 5464 da (measured by GPC). IR (KBr) ν, 3315, 3087, 2923, 2845, 1747, 1535, 1426, cm^{-1}. ^{1}H NMR (400 MH_Z, DMSO, δ ppm): 7.60 (s, 2H), 6.47 (m, 4H), 5.92 (s, 2H), 3.06 (s, 4H), 2.86 (m, 8H), 1.34 (m, 4H), 1.17 (m, 6H).

Synthesis of crosslinked polymer CP_2 from the linear LP_2 and *N,N′*-4,4′-diphenylmethyene bismaleimide (BMI) through Diels–Alder [4 + 2] cycloaddition reaction

The polymer $\mathbf{CP_2}$ was prepared by the method similar to that of $\mathbf{CP_1}$ [36]. The linear oligomer $\mathbf{LP_2}$ (528 mg), *N,N´*-4,4´-diphenylmethyene bismaleimide (BMI) (360 mg) and 1,4-dioxane (5 mL) were sequentially added to a three-necked 25 mL flask, and the mixture was stirred at 80 °C for 16 h under N_2 atmosphere in a dark place. Then, part of the mixture was coated on a glass substrate to form a film. The left part was continued stirring for another 32 h to obtain brown gel-like polymer $\mathbf{CP_2}$ (471 mg, c.a. 53%). The glass transition temperature (T_g) of $\mathbf{CP_2}$ was 7.00 °C. IR (KBr) ν: 3307, 2931, 2845, 1774, 1718, 1401 cm^{-1}.

Determination of medium resistance of the crosslinked polymers

The film mass of the crosslinked polymer was measured on a balance, and the film was dipped in different media, 1 mol/L aqueous HCl, 1 mol/L aqueous NaOH, THF, toluene, EtOH, and deionized water for 5 days. The film sample was dried in an oven and its mass was measured again. Medium resistance of the crosslinked polymer can be evaluated according to mass loss of the film. The lower mass loss of the film, stronger is the medium resistance of the crosslinked polymer.

Determination of gel fraction of the crosslinked polymers

Gel fraction was measured by modifying the method reported in literature [37, 38]. About 350 mg of a sample $\mathbf{CP_1}$ or $\mathbf{CP_2}$ was weighed accurately, and the mass was noted as W_0. Then the sample was packed by a steel wire mesh (120 mesh) and extracted with xylene in Soxhlet for 10 h. The sample was taken out and washed with ethanol, followed by drying at 140 °C for 4 h. The sample was weighed accurately again, and the mass was noted as *W*. Gel fraction was calculated as $G\,(\%) = (W/W_0) \times 100$.

Determination of self-healing performance of the crosslinked polymers

Method 1: a film of crosslinked polymer was cut to form a crack by a razor. The crack of the film was photographed by a Japanese JSM-6701F cold field emission scanning electron microscope. Then the injured film was heated at 50 °C in an oven for 3 h, and photographed again to observe self-healing state. Thus, the film was at 50 °C in an oven for another 5 h, and photographed again to observe self-healing state. The self-healed film was cut again in the same place and placed in an oven at 50 °C for 12 h, and photographed again to observe re-self-healing performance. **Method 2**: stress–strain curves of original film and self-healed film were compared.

Results and discussion

Synthesis and characterization of polymers

Synthesis of 1,6-diisocyanohexane (1)

There are usually two steps for the synthesis of isocyanides: the first step is preparation of *N*-substituted formamides from ethyl formate and free amines; the second is synthesis of isocyanides by appropreiate acidic dehydrating agens, such as phosphorous oxychloride and *para*-tosyl chloride [39]. Thus, 1,6-diaminohexane was converted to the corresponding diformamides, followed by adding phosphorous oxychloride to obtain 1,6-diisocyanohexane (**1**) in 76% yield. The ^{1}H NMR spectrum of **1** is shown in Fig. 1. The peak at chemical shift of 3.43–3.37 ppm (marked as "a") is signal of protons of two methylene groups adjacent to isocyanate groups. The other two peaks at 1.75–1.65 ppm and 1.55–1.45 ppm represent eight protons signals of the rest four methylene groups (marked as "b" and "c", respectively).

Synthesis and characterization of the linear polymer LP_1

Passerini three-component reaction (Passerini 3-CR) can be conducted easily by mixing an appropriate amine, carboxylic acid and isocyanide without any other catalysts or additives, which is unambiguously an atom-economic reaction. In order to utilize renewable materials from biomass or renewable platform chemicals, we deliberately chose furfural, adipic acid, and 1,6-diisocyanohexane (**1**) as reactants to synthesize $\mathbf{LP_1}$ (Scheme 1). Furfural can be produced directly from biomass such as corn cob or rice husk [40, 41]. Adipic acid may be potentially prepared from renewable platform chemicals such as glucaric acid or mucic acid [42–44]. 1,6-Diisocyanohexane (**1**) has been synthesized from 1,6-diaminohexane, while 1,6-diaminohexane may be prepared from adipic acid. Thus, after furfural, adipic acid, and 1,6-diisocyanohexane (**1**) were mixed and stirred for hours, the resulting linear polymer $\mathbf{LP_1}$ could be collected through precipitation and filtration by adding poor solvent petroleum ether. The ^{1}H NMR spectrum of $\mathbf{LP_1}$ is illustrated in Fig. 2. The peaks (marked as "c, e and d") at 7.41 ppm, 6.37 ppm, 6.19 ppm are signal of protons on aryl ring of furans, and the signal at 6.50 ppm (designated as "f") can be attributed to protons of methylene group of furfural. Ratio of the four kinds of protons is almost 1:1:1:1, indicating that Passerini reaction product was formed. The peak at 3.30 ppm (marked as "h") may be the protons of methylene groups connected with nitrogen atoms, while that at 2.93 ppm (marked as "a") may be contributed by protons of methylene groups close to ester groups. Number-average molecular weight of $\mathbf{LP_1}$ (M_{nLp1}) is 2189 da. The molecular weight of one repeating unit of $\mathbf{LP_1}$ is 474.5, so degree of polymerization (DP) is about 4.6, i.e., $n = 4.6$.

The FTIR spectrum of the linear polymer $\mathbf{LP_1}$ is shown in Fig. 3A-a. The peak at 3340 cm^{-1} is stretching vibration of amide N–H, and the strong peak at 1754 cm^{-1} means stretching vibration of carbonyl groups. At 3081 cm^{-1}, the weak peak may be C–H stretching vibration of furan rings. The peaks at 2931 and 2852 cm^{-1} represent C–H stretching vibration of methylene groups.

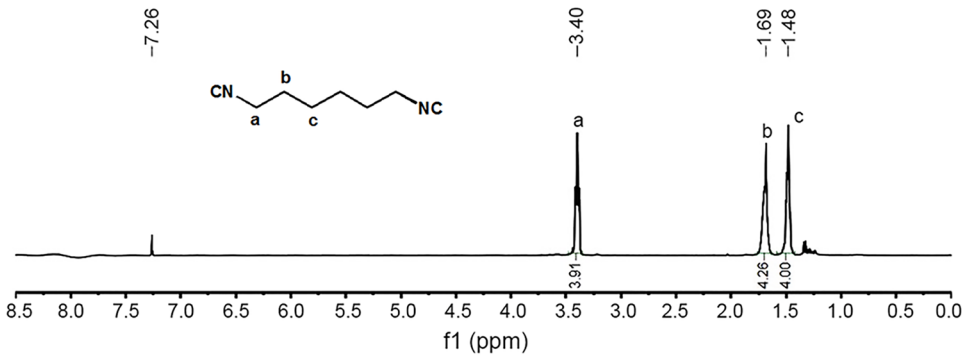

Fig. 1 ^{1}H NMR spectrum of 1,6-diisocyanohexane (**1**)

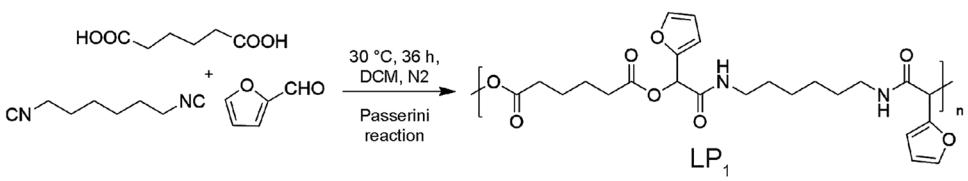

Scheme 1 Synthesis of linear polymer $\mathbf{LP_1}$ through Passerini reaction

Synthesis and characterization of the crosslinked polymer CP_1

There are side furan rings in the linear pre-polymer $\mathbf{LP_1}$ as shown in Schemes 1 and 2. These furan rings in $\mathbf{LP_1}$ as electron-efficient diene can easily proceed Diels–Alder [4 + 2] cycloaddition reaction with electron-deficient dienophile such as BMI, which produces the crosslinked polymer $\mathbf{CP_1}$ as illustrated in Scheme 2. When the molar ratio of BMI and repeating unit of $\mathbf{LP_1}$ is being controlled to be 1:1, gelation phenomenon would occur after the reaction had been conducted for 48 h, causing inconvenience for manipulation

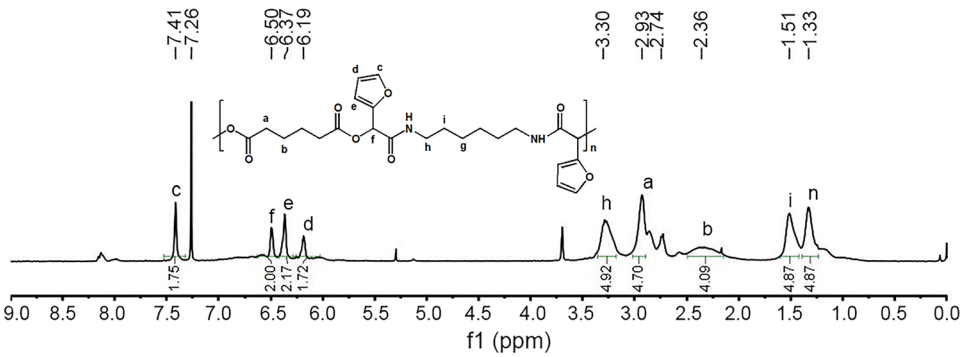

Fig. 2 ^{1}H NMR spectrum of linear polymer $\mathbf{LP_1}$

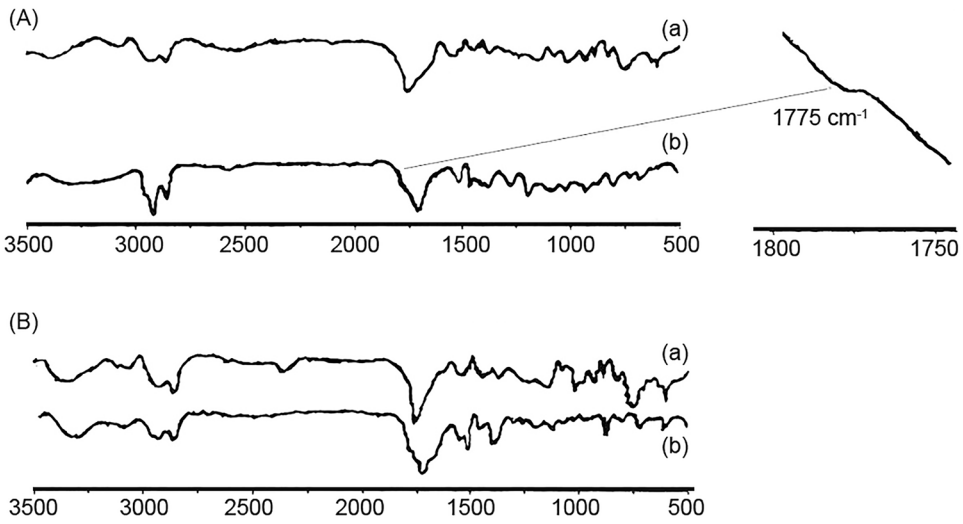

Fig. 3 **A** FTIR spectra of **a** $\mathbf{LP_1}$ linear polymer, and **b** $\mathbf{CP_1}$ crosslinked polymer; **B** FTIR spectra of: **a** $\mathbf{LP_2}$ linear polymer, and **b** $\mathbf{CP_2}$ crosslinked polymer

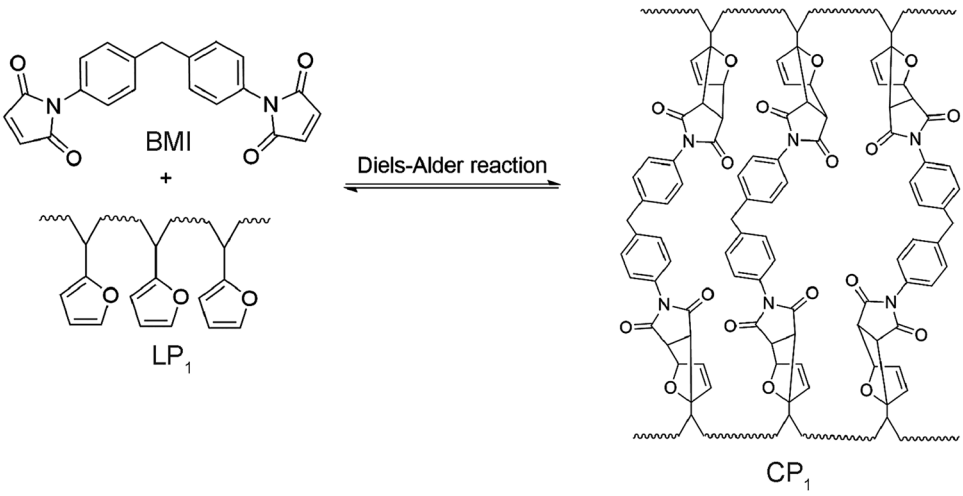

Scheme 2 Synthesis of crosslinked polymer $\mathbf{CP_1}$ from $\mathbf{LP_1}$ and BMI through Diels–Alder reaction

of samples. Therefore, when the reaction proceeded for 10 h, the mixture was coated on a glass substrate to form a film for measuring other properties. The images of gel sample and film sample of $\mathbf{CP_1}$ are demonstrated in Fig. 4.

The structure of $\mathbf{CP_1}$ is further confirmed by FTIR spectrum (Fig. 3A-b). A very weak peak appears at 1775 cm^{-1}, indicating the formation of new carbon–carbon double bonds in the previous furan rings through Diels–Alder reaction [36]. The peaks at the wavenumber of 2931 and 2845 cm^{-1} are C–H stretching vibration of methylene groups. The strong peak at 1741 cm^{-1} corresponds to the stretching vibration of carbonyl groups. Several peaks from 1548 to 1505 cm^{-1} stems from benzene skeleton vibration. At 1407 cm^{-1}, there appears the signal of amide C–N stretching vibration.

Synthesis and characterization of linear polymer LP_2 and crosslinked polymer CP_2

Healing ability and reliability of materials may be promoted by introducing two or more kinds of dynamic bonds [45]. Dynamic disulfide or multi-sulfide bonds are usually applied in designing functional materials including self-healing or reprocessable polymers [46–48]. These inspired us to utilize 3,3´-dithiodipropionic acid, a diacid with a disulfide group, to replace adipic acid in Passerini reaction for preparing the linear polymer $\mathbf{LP_2}$ (Scheme 3). The reaction was carried out in a similar way as preparation of $\mathbf{LP_1}$. The ^{1}H NMR spectroscopy (DMSO-D_6 as the solvent) of $\mathbf{LP_2}$ is illustrated in Fig. 5. Two peaks at the chemical shift of 7.60 and 6.47 ppm are signals of six protons on two furan rings. The signals of protons of methyne that is connected with a furan ring, an oxygen and a carbonyl group appear at 5.92 ppm. The peak at 3.06 ppm is attributed to methylene groups connected to nitrogen atom. The four methylene groups from

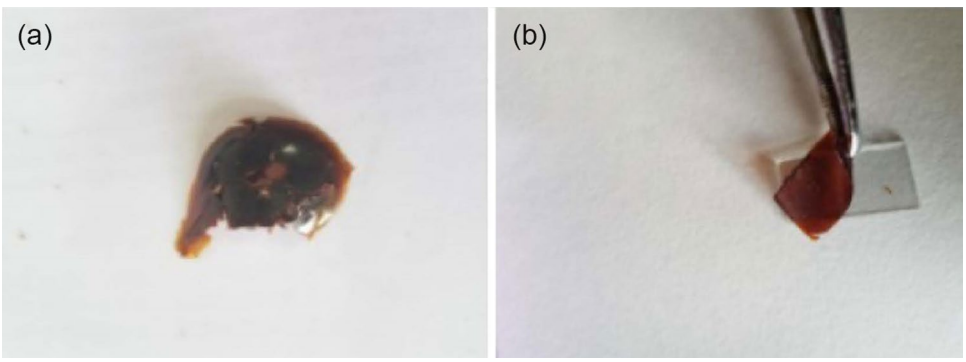

Fig. 4 Two forms of the crosslinked polymer $\mathbf{CP_1}$: (a) gel state, and (b) a film on glass substrate

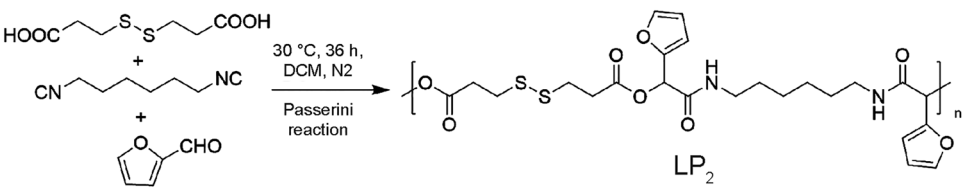

Scheme 3 Synthesis of linear polymer $\mathbf{LP_2}$ through Passerini reaction

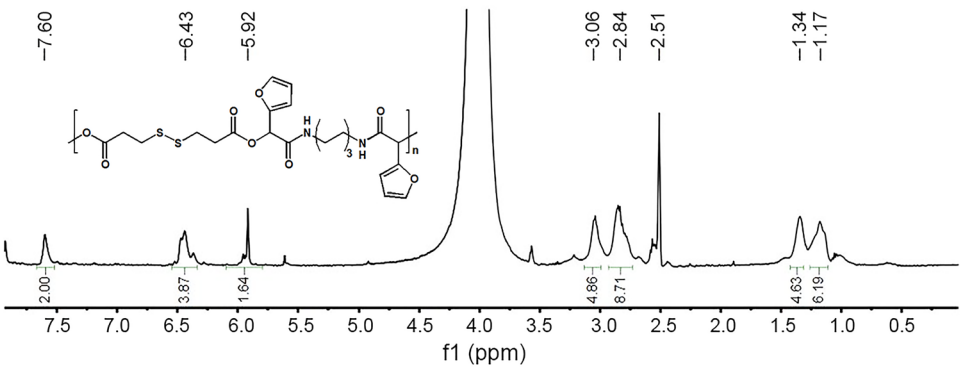

Fig. 5 ^{1}H NMR spectrum of the linear polymer $\mathbf{LP_2}$

3,3'-dithiodipropionic acid ester give a signal at 2.84 ppm. Protons of all the other methylene groups produced peaks at 1.34 and 1.17 ppm, respectively.

The FTIR spectrum of **LP_2** is demonstrated in Fig. 3B-a. The broad peak at 3315 cm^{-1} is attributed to stretching vibration of amide N–H bond. The peak at 3087 cm^{-1} results from the C–H stretching vibration of aromatic furan rings. Signals at 2923 and 2845 cm^{-1} correspond to the C–H stretching vibration of methylene groups in the main chain. The strong peak at 1747 cm^{-1} is a signal of carbonyl groups. The C–N stretching vibration of amide groups gives a peak at 1426 cm^{-1}.

The crosslinked polymer **CP_2** was prepared through Diels–Alder reaction between **LP_2** and BMI in a similar way as that of **CP_1**. The FTIR spectrum of **CP_2** is shown in Fig. 3B-b, and the characteristic peak at 1774 cm^{-1} confirms successful Diels–Alder crosslinking reaction.

Properties of the crosslinked polymers CP_1 and CP_2

Chemical resistance of CP_1 and CP_2

Chemical corrosion is sometimes unavoidable during application of polymer materials (e.g., rubber gasket in chemical reaction kettle). Therefore, measurement of chemical resistance is necessary. Herein, we only evaluate the chemical resistance property from relative mass loss after dipping samples into chemical media for a period of time. Related relative mass loss data of **CP_1** and **CP_2** are shown in Table 1. We selected five typical chemical media including strong acids, strong bases, and good solvents. The polymer **CP_1** has relatively good resistance to acid, ethyl acetate and toluene, but relatively poor resistance to base and THF. The polymer **CP_2** has relatively good resistance to acid and ethyl acetate. By comparison, chemical resistance performance of **CP_1** is better than that of **CP_2**, which may be due to the existence of relatively weak disulfide bonds in **CP_2**.

Gel fraction of CP_1 and CP_2

Gel fraction may reflect crosslinking state of thermoset polymers. Gel fraction of **CP_1** was determined to be 82%, while that of **CP_2** was 74%. This means that most of linear segments of **LP_1** and/or **LP_2** were crosslinked. We think that the measured values may be lower than the real values as it was in favor of reverse reaction (i.e., depolymerization reaction) under heating conditions during measurement. The value of **CP_1** was higher than that of **CP_2**, which may be explained that **CP_2** has undergone both reverse D–A reaction and reverse disulfide-bond-cleavage/reshuffling, leading to lower gel fraction values.

Table 1 Chemical resistance of the crosslinked polymers **CP_1** and **CP_2**

Sample	Chemical media[a]	m_1/mg[c]	m_2/mg[c]	Δm/mg[c]	Relative mass loss (%)[c]
CP_1	HCl	358.2	357.5	0.7	0.19
	NaOH	321.5	319.7	1.8	0.55
	THF	300.3	297.2	3.1	1.00
	EA	379.2	378.5	0.7	0.18
	Tol	386.5	385.4	1.1	0.28
CP_2	HCl	412.5	411.8	0.7	0.16
	NaOH	365.4	364.3	1.1	0.84
	THF	356.8	352.9	3.9	1.09
	EA	329.7	328.4	0.7	0.21
	Tol	319.8	317.6	2.2	0.68

All the polymer samples were dipped into the medium for 5 days under ambient conditions

EA ethyl acetate, *Tol.* means toluene

[a] m_1: mass of sample before dipping; m_2: mass of sample after being dipped in medium for 5 days; relative mass loss (%) = $[(m_1 - m_2)/m_1] \times 100$. [c] Chemical media: HCl means 1 mol L^{-1} aqueous HCl; NaOH means 1 mol L^{-1} aqueous NaOH

Thermal properties of CP_1 and CP_2

Glass transition temperatures of **CP_1** and **CP_2** are $T_{gCP1} = 14.78$ ℃ and $T_{gCP2} = 7.00$ ℃, respectively, indicating that both polymers are at rubbery state. Heat resistance of the polymers was determined by thermogravimetric analysis (TGA)-derivative thermogravimetry (DTG) (Fig. 6a, b). TGA diagram of the polymer **CP_1** is demonstrated in Fig. 6a. Td_{10} value is about 151 ℃, meaning that small molecular impurities such as water are volatile at this temperature. The first decomposition peak value appears at about 210 ℃, indicating that monomer or oligomer residues are decomposed or rapidly volatile at this temperature. Td_{50} value is about 420 ℃. The TGA diagram of **CP_2** is shown in Fig. 6b. Its Td_{10} value is about 131 ℃, and the first decomposition peak occurs at about 150 ℃. Td_{50} value is about 397 ℃. By comparing **CP_1** and **CP_2**, heat resistance of **CP_1** is higher than that of **CP_2**, presumably because the polymer **CP_2** contains relatively weak disulfide bonds.

Self-healing behavior of CP_1 and CP_2

Diels–Alder reaction is reversible and can be used to prepare versatile functional polymer materials [49, 50]. Among them, thermally triggered self-healable polymers were also prepared through this strategy [36, 51]. The thermosets **CP_1** as well as **CP_2** were also crosslinked by Diels–Alder reaction, and expected to have healable behavior. Thus, firstly, we tested healing property of **CP_1** under appropriate thermal

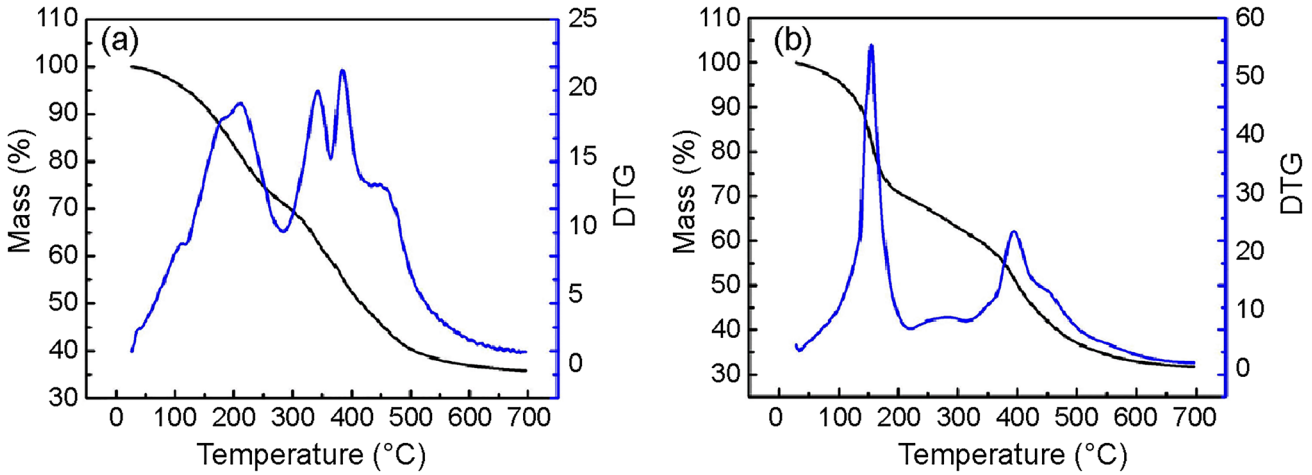

Fig. 6 TGA-DTG diagrams of: **a** $\mathbf{CP_1}$ polymer and **b** $\mathbf{CP_2}$ polymer

conditions. Film samples of $\mathbf{CP_1}$ were cut by a razor to form scratches, and the "injured" samples were then heated at temperatures of 40, 50, 60, 70, 80, 90, 100 °C for different times. To our joy, the samples showed self-healing property at the temperature of 60 °C or higher. Compared to high temperatures, longer time was required for healing process at the temperature as low as 60 °C. This may be explained as follows: (i) main chain of $\mathbf{CP_1}$ is composed of flexible alkyl monomers, which makes the wounded part "flow or move" more easily at temperatures close to or higher than T_g temperature (14.78 ℃); (ii) retro-Diels–Alder reactions were usually endothermic, and it is slow to build dynamic balance between Diels–Alder and retro-Diels–Alder reactions at relatively low temperatures such as 60 °C [36]. Yet, we chose the temperature of 60 °C to explore healing behavior of $\mathbf{CP_1}$ in order to save energy. First, a sample of $\mathbf{CP_1}$ was cut for the first time by a razor to form a scratch (Image 1, Fig. 7). Then, the scratched sample was heated in an oven at 60 °C for 3 h, and the scratch was partially healed as shown in Image 2 of Fig. 7. Then, the partially healed sample was continued to be heated at 60 °C for another 5 h, and the sample was almost completely self-repaired (Image 3, Fig. 7). The healed sample was cut again at the same site as that of the first time (Image 4, Fig. 7), and then the second cut sample was placed in an oven at 60 °C for 24 h. The sample was self-healed again (Image 5, Fig. 7), meaning that the intrinsic self-healing polymer $\mathbf{CP_1}$ could self-heal more than once.

Next, we evaluated the healing percentage by comparing stress–strain properties of an initial uncut sample and the second-time healing $\mathbf{CP_1}$ sample. As shown in Fig. 8a, the largest stress of the initial uncut sample is 0.37 MPa while the largest strain can reach more than 100%, indicating that $\mathbf{CP_1}$ has good elastomeric property. Young's modulus of $\mathbf{CP_1}$ is 0.35 MPa. For the second-time healing sample, the largest stress is about 0.20 MPa (Fig. 8b). Thus, the healing percentage may be calculated as follows: 0.20/0.37 = 54.1%. Young's modulus of the healed $\mathbf{CP_1}$ is 0.23 MPa.

There are two kinds of dynamic covalent bonds in the polymer $\mathbf{CP_2}$, which is expected to own thermo- and light-dual stimuli response behavior. In a similar manner as that of $\mathbf{CP_1}$, the $\mathbf{CP_2}$ sample was cut and heated at 60 °C for 24 h, and after that the cut mark disappeared completely (Fig. 9). Then, we explored healing behavior of $\mathbf{CP_2}$ under UV light irradiation conditions. A sample of $\mathbf{CP_2}$ was wounded by a razor (Fig. 10a), followed by irradiation under UV light with 360 nm wavelength. To our surprise, the scratched sample was partially healed within only 3 min (Fig. 10b), and the partially healed sample was completely healed after being irradiated by UV for another 7 min. That is to say, the scratched sample can be completely healed within 10 min (Fig. 10c). The rapid healing behavior under UV light may be contributed to both dynamic disulfide bonds and dynamic D–A bonds, as the temperature of the $\mathbf{CP_2}$ sample also rose under UV light. The healed sample was cut again and self-healed for the second time after being irradiated under UV for 30 min (Fig. 10d, e).

Mechanical properties of $\mathbf{CP_2}$ were also studied by testing stress–strain correlation. As shown in Fig. 11, (**a**) is the stress–strain curve of an initial $\mathbf{CP_2}$ sample, and the maximal stress is 0.33 MPa while the maximal strain can reach 125%. Thus, Young's modulus of $\mathbf{CP_2}$ is calculated to be 0.26 MPa; (**b**) is the stress–strain curve of the UV-triggering self-healed $\mathbf{CP_2}$ sample, which provides 0.21 MPa of maximal stress and 60% of maximal strain (Young's modulus of the healed $\mathbf{CP_2}$ is 0.35 MPa). Thus, the healing percent is: 0.21/0.33 = 63.6%. In contrast, the healing percent of $\mathbf{CP_2}$ (63.6%) is higher than that of $\mathbf{CP_1}$ (54.1%), which may be ascribed to dual dynamic bonds of $\mathbf{CP_2}$ that causes more efficient self-healing process.

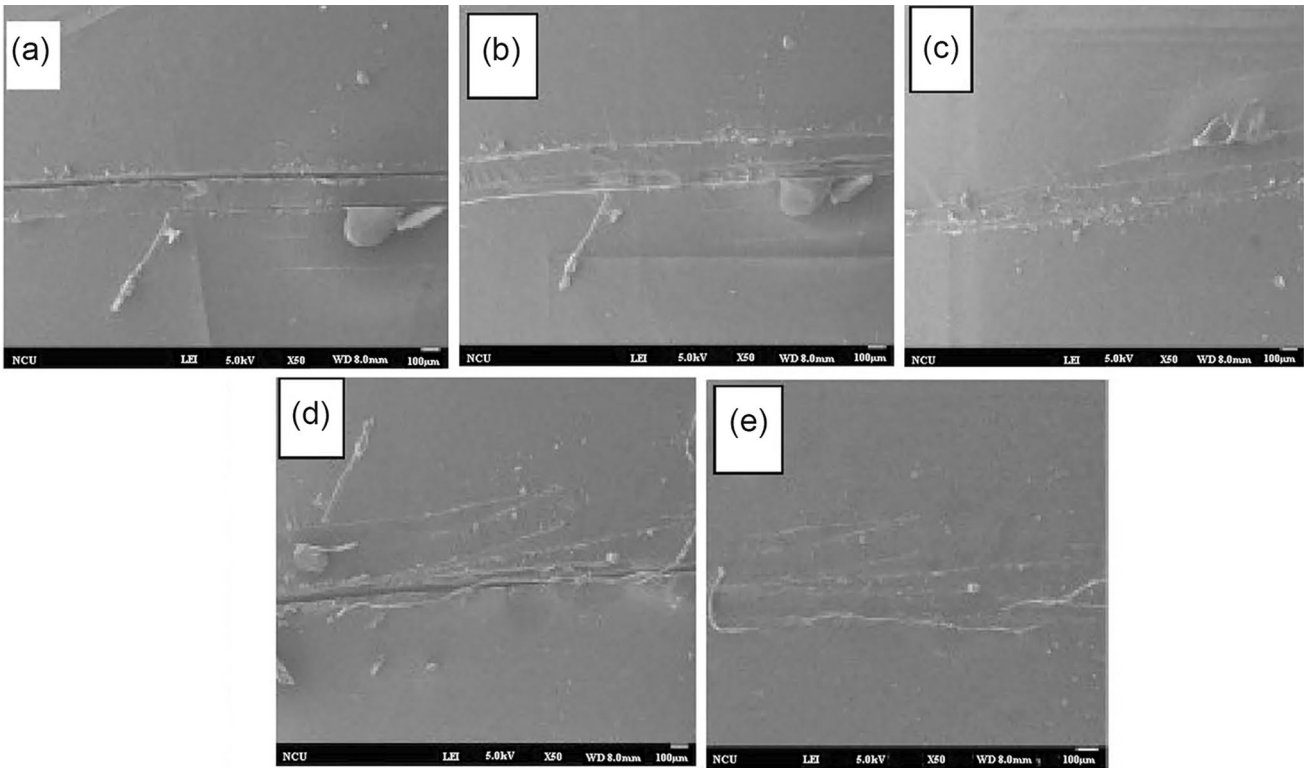

Fig. 7 SEM images of self-healing process of the thermoset $\mathbf{CP_1}$. Image 1: A film of $\mathbf{CP_1}$ sample was cut by a razor to form a scratch**;** Image 2: the scratched sample (Image 1) was partially healed after being heated at 60 °C for 3 h; Image 3: the partially healed sample (Image 2) was heated at 60 °C for another 5 h and was almost "completely" self-healed; Image 4: the "completely" healed sample (Image 3) was cut by a razor again at the same position of the sample as that of Image 1; Image 5: the cut sample (Image 4) was healed again after being heated at 60 °C for 24 h

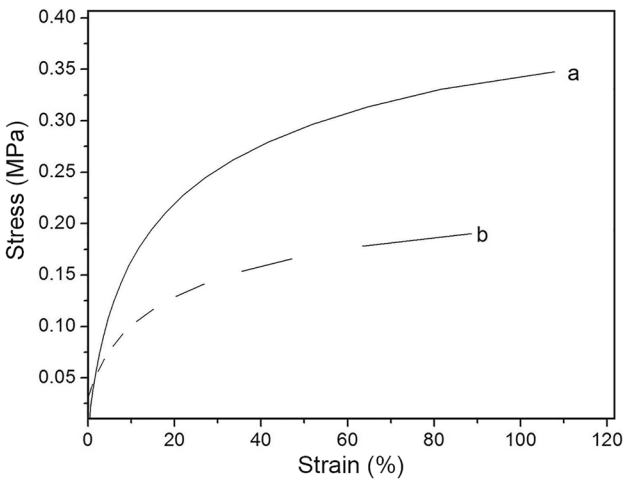

Fig. 8 Curves of stress–strain: **a** the initial uncut $\mathbf{CP_1}$ sample, and **b** the second-time healing $\mathbf{CP_1}$ sample

Conclusion

Two linear polymers $\mathbf{LP_1}$ and $\mathbf{LP_2}$ were synthesized by highly efficient Passerini three-component reactions from materials based on platform chemicals. Among them, $\mathbf{LP_1}$ was even prepared from fully bio-based platform chemicals, i.e., furfural, adipic acid and 1,6-hexadiamine. $\mathbf{LP_2}$ was produced from furfural, 3,3´-dithiodipropionic acid and 1,6-hexadiamine. The structure of $\mathbf{LP_1}$ and $\mathbf{LP_2}$ was confirmed by ^{1}H NMR as well as FTIR spectra. The number-average molecular weights of $\mathbf{LP_1}$ and $\mathbf{LP_2}$ are 2189 da and 5464 da, respectively. There are pedant furan side groups in both $\mathbf{LP_1}$ and $\mathbf{LP_2}$, which make them successfully undergo Diels–Alder crosslinking reaction with BMI. Two dynamically crosslinked networks $\mathbf{CP_1}$ and $\mathbf{CP_2}$ were prepared by this crosslinking reaction. The structures of $\mathbf{CP_1}$ and $\mathbf{CP_2}$ were verified by appearance of a weak peak at around 1775 cm^{-1} in FTIR spectra. Gel fraction of $\mathbf{CP_1}$ was determined to be 82%, while that of $\mathbf{CP_2}$ was 74%, which indicated that most of linear segments of $\mathbf{LP_1}$ and/or $\mathbf{LP_2}$ were crosslinked. Both of $\mathbf{CP_1}$ and $\mathbf{CP_2}$ showed good resistance to acid, and ethyl acetate, but relatively poor resistance to base and THF. The T_g values of $\mathbf{CP_1}$

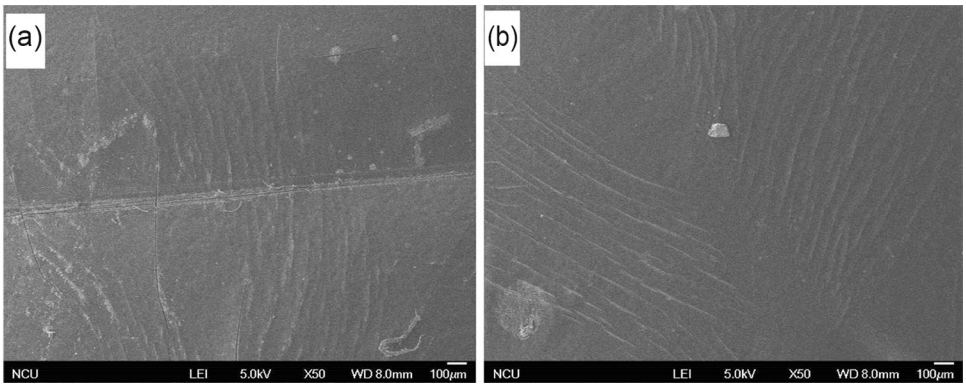

Fig. 9 SEM images of self-healing process of the thermoset $\mathbf{CP_2}$ under heating conditions: (**1**) A film of $\mathbf{CP_2}$ sample was cut to form a scratch, and (**2**) the scratched sample was "completely" restored after being heated at 60 °C for 24 h

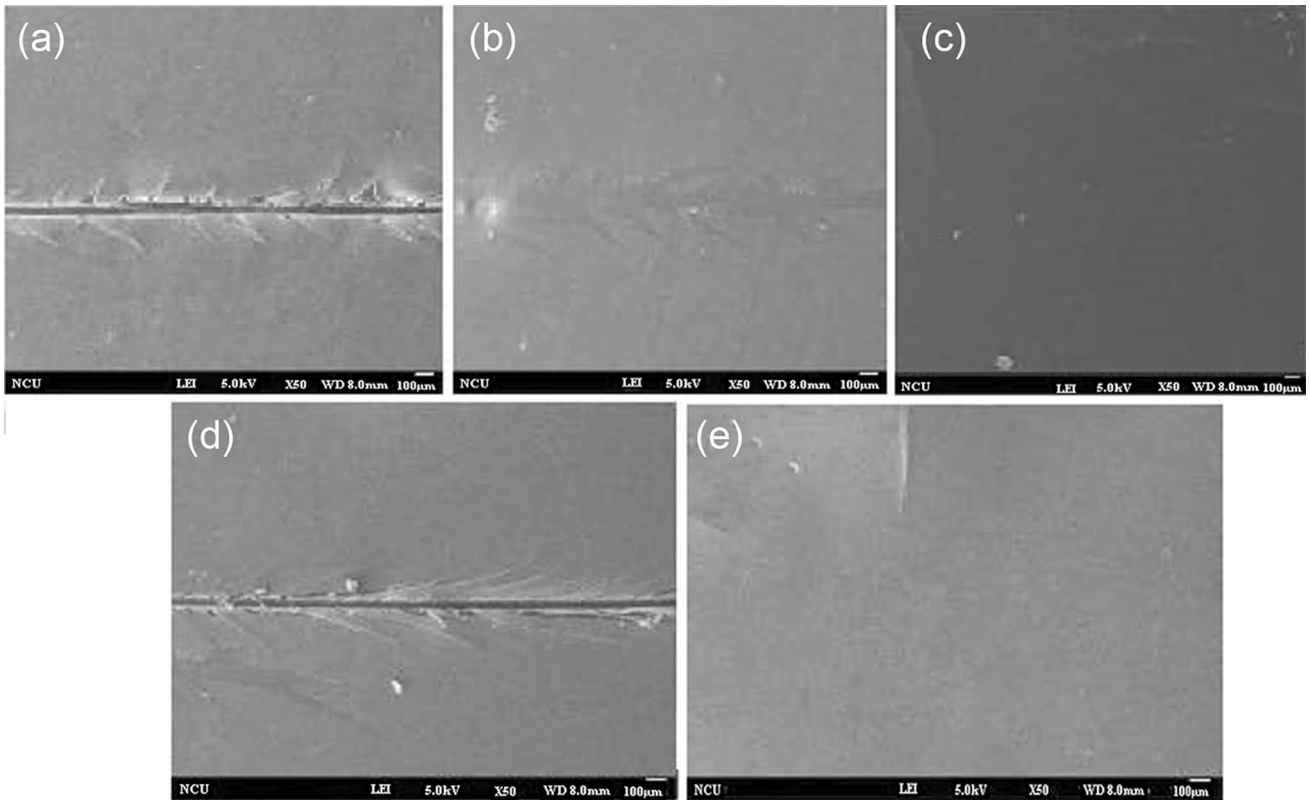

Fig. 10 SEM images of self-healing process of the thermoset $\mathbf{CP_2}$ under UV light (wavenumber 360 nm) irradiation conditions: **a** a film of $\mathbf{CP_2}$ sample was cut to form a scratch; **b** the scratched sample was partially healed after being irradiated by UV light for 3 min; **c** the partially healed sample was completely healed after being further irradiated for another 7 min; **d** the healed sample was cut again at the same place as that of the first time; **e** the secondly cut sample was healed for the second time after being irradiated under UV for 30 min

and $\mathbf{CP_2}$ are 14.78 ℃ and 7.00 ℃, respectively. From TGA-DTG analysis data, Td_{10} of $\mathbf{CP_1}$ is 151 °C, while that of $\mathbf{CP_2}$ is 131 °C, indicating that heat resistance of $\mathbf{CP_1}$ is higher than that of $\mathbf{CP_2}$, presumably because the polymer $\mathbf{CP_2}$ contains relatively weak disulfide bonds. At 60 °C or higher temperatures, both of $\mathbf{CP_1}$ and $\mathbf{CP_2}$ demonstrated thermo-stimulus self-healing behavior, though the healing process required hours at 60 °C. Furthermore, $\mathbf{CP_2}$ showed rapid self-healable property under 360 nm UV irradiation within 10 min, because there are dynamic disulfide bonds in $\mathbf{CP_2}$. By determining and comparing maximal stress, the healing percent of $\mathbf{CP_2}$ (63.6%) is higher than that of $\mathbf{CP_1}$ (54.1%), which may be ascribed to dual dynamic bonds of $\mathbf{CP_2}$ that causes more efficient self-mending process. Our work provides a simple method for designing and preparing self-healable polymers from renewable platform chemicals.

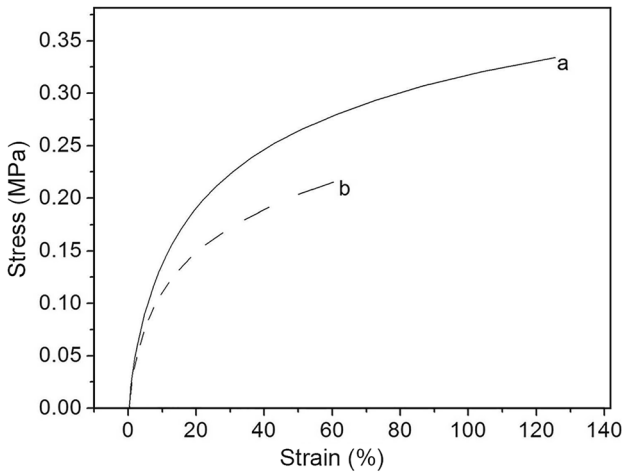

Fig. 11 Curves of stress–strain: **a** the initial uncut $\mathbf{CP_2}$ sample, and **b** the second-time healing $\mathbf{CP_2}$ sample

Supplementary Information The online version contains supplementary material available at https://doi.org/10.1007/s13726-023-01206-4.

Acknowledgements The work was financially supported by Natural Science Foundations of China (No. 21564004).

References

1. Yang E, Miao S, Zhong J, Zhang ZY, Mills DK, Zhang LJG (2018) Bio-based polymers for 3D printing of bioscaffolds. Polym Rev 58:668–687
2. Kargarzadeh H, Mariano M, Huang J, Lin N, Ahmad I, Dufresne A, Thomash S (2017) Recent developments on nanocellulose reinforced polymer nanocomposites: a review. Polymer 132:368–393
3. Cheng CJ, Li YP, Zhang X, Li J (2017) Eugenol-based non-isocyanate polyurethane and polythiourethane. Iran Polym J 26:821–831
4. Wang XZ, Xia QQ, Jing SS, Li C, Chen QY, Chen B, Pang ZQ, Jiang B, Gan WT, Chen G, Cui MJ, Hu LB, Li T (2021) Strong, hydrostable, and degradable straws based on cellulose-lignin reinforced composites. Small 17:2008011
5. Wang SC, Bai JX, Innocent MT, Wang QQ, Xiang HX, Tang JG, Zhu MF (2022) Lignin-based carbon fibers: formation, modification and potential applications. Green Energy Environ 7:578–605
6. Jaswal A, Singha PP, Mondal T (2022) Furfural: a versatile, biomass-derived platform chemical for the production of renewable chemicals. Green Chem 24:510–551
7. Luo YP, Li Z, Li XL, Liu XF, Fan JJ, Clark JH, Hu CW (2019) The production of furfural directly from hemicellulose in lignocellulosic biomass: a review. Catal Today 319:14–24
8. Putten RJ, Waal JC, Jong E, Rasrendra CB, Heeres HJ, Vries JG (2013) Hydroxymethylfurfural: a versatile platform chemical made from renewable resources. Chem Rev 113:1499–1597
9. Papageorgiou GZ, Papageorgiou DG, Terzopoulou Z, Bikiaris DN (2016) Production of bio-based 2,5-furan dicarboxylate polyesters: recent progress and critical aspects in their synthesis and thermal properties. Eur Polym J 83:202–229
10. Xiang YP, Wen S, Tian Y, Zhao KY, Guo DW, Cheng F, Xu Q, Liu XX, Yin DL (2021) Efficient synthesis of 5-ethoxymethylfurfural from biomass-derived 5-hydroxymethylfurfural over sulfonated organic polymer catalyst. RSC Adv 11:3585–3595
11. Xu ZW, Yan PF, Liu KR, Wan L, Xu WJ, Li HX, Liu XM, Zhang ZC (2016) Synthesis of bis(hydroxylmethylfurfuryl)amine monomers from 5-hydroxymethylfurfural. Chemsuschem 9:1255–1258
12. Kieber RJ III, Silver SA, Kennemur JG (2017) Stereochemical effects on the mechanical and viscoelastic properties of renewable polyurethanes derived from isohexides and hydroxymethylfurfural. Polym Chem 8:4822–4829
13. Zhang Q, Wang XY, Cheng CJ, Zhu R, Liu N, Hu YF (2012) Copper(I) acetate–catalyzed azide-alkyne cycloaddition for highly efficient preparation of 1-(pyridin-2-yl)-1,2,3-triazoles. Org Biomol Chem 10:2847–2854
14. Zhao Y, Wu HB, Wang ZL, Wei Y, Wang ZM, Tao L (2016) Training the old dog new tricks: the applications of the Biginelli reaction in polymer chemistry. Sci Chin Chem 59:1541–1547
15. Filho JFA, Lemos BC, Souza AS, Pinheiro S, Greco SJ (2017) Multicomponent Mannich reactions: general aspects, methodologies and applications. Tetrahedron 73:6977–7004
16. Rocha RO, Rodrigues MO, Neto BAD (2020) Review on the Ugi multicomponent reaction mechanism and the use of fluorescent derivatives as functional chromophores. ACS Omega 5:972–979
17. Singh K, Kaur A, Mithu VS, Sharma S (2017) Metal-free organocatalytic oxidative Ugi reaction promoted by hypervalent iodine. J Org Chem 82:5285–5293
18. Ashjari M, Garmroodi M, Ahrari F, Yousefi M, Mohammadi M (2020) Soluble enzyme cross-linking via multi-component reactions: a new generation of cross-linked enzymes. Chem Commun 56:9683–9686
19. Xu J, Fan WG, Popowycz F, Queneau Y, Gu YH (2019) Multicomponent reactions: a new strategy for enriching the routes of value-added conversions of bio-platform molecules. Chin J Org Chem 39:2131–2138
20. Kayser LV, Vollmer M, Welnhofer M, Krikcziokat H, Meerholz K, Arndtsen BA (2016) A metal-free, multicomponent synthesis of pyrrole-based-conjugated polymers from imines, acid chlorides and alkynes. J Am Chem Soc 138:10516–10521
21. Xue HD, Zhao Y, Wu HB, Wang ZL, Yang B, Wei Y, Wang ZM, Tao L (2016) Multicomponent combinatorial polymerization via the Biginelli reaction. J Am Chem Soc 138:8690–8693
22. Xu LG, Zhou F, Liao M, Hu RR, Tang BZ (2018) Room temperature multicomponent polymerizations of alkynes, sulfonyl azides, and *N*-protected isatins toward oxindole-containing poly(*N*-acylsulfonamide)s. Polym Chem 9:1674–1683
23. Wang X, Liu C, Xing ZH, Suo HY, Qu R, Li QZ, Qin YS (2022) Furfural-based polyamides with tunable fluorescence properties via Ugi multicomponent polymerization. Macromolecules 55:8857–8865
24. Bode ML, Gravestock D, Rousseau AL (2016) Synthesis, reactions and uses of isocyanides in organic synthesis. Org Prep Proced Int 48:89–221
25. Liu JP, Luo ZL, Yu L, Zhang P, Wei HQ, Yu Y (2020) A new soft-matter material with old chemistry: Passerini multicomponent polymerization-induced assembly of AIE-active double-helical polymers with rapid visible-light degradability. Chem Sci 11:8224–8230
26. Zhang XJ, Wang SX, Liu J, Xie ZG, Luan SF, Xiao CS, Tao YH, Wang XH (2016) Ugi reaction of natural amino acids: a general route toward facile synthesis of polypeptoids for bioapplications. ACS Macro Lett 5:1049–1054
27. Cui Y, Zhang M, Du FS, Li ZC (2017) Facile synthesis of H_2O_2-cleavable poly(ester-amide)s by Passerini multicomponent polymerization. ACS Macro Lett 6:11–15
28. Zhang Q, Zhang YN, Wan Y, Carvalho W, Hu L, Serpe MJ (2021) Stimuli-responsive polymers for sensing and reacting to environmental conditions. Prog Polym Sci 116:101386

29. Bauri K, Nandi M, De P (2018) Amino acid-derived stimuli-responsive polymers and their applications. Polym Chem 9:1257–1287
30. Yang P, Zhu F, Zhang ZB, Cheng YY, Wang Z, Li YW (2021) Stimuli-responsive polydopamine-based smart materials. Chem Soc Rev 50:8319–8343
31. Zhou Y, Li L, Han ZB, Li Q, He JL, Wang Q (2023) Self-healing polymers for electronics and energy devices. Chem Rev 123:558–612
32. Yu XH, Zhang HP, Wang YF, Fan XS, Li ZB, Zhang X, Liu TX (2022) Highly stretchable, ultra-soft, and fast self-healable conductive hydrogels based on polyaniline nanoparticles for sensitive flexible sensors. Adv Funct Mater 32:2204366
33. Wang MY, Zhuge JP, Li CQ, Jiang LB, Yang H (2020) Self-healing quadruple shape memory hydrogels based on coordination, borate bonds and temperature with tunable mechanical properties. Iran Polym J 29:569–579
34. Gulevich AV, Koroleva LS, Morozova OV, Bakhvalova VN, Silnikov VN, Nenajdenko VG (2011) Multicomponent synthesis of artificial nucleases and their RNase and DNase activity. Beilstein J Org Chem 7:1135–1140
35. Wang YZ, Deng XX, Li L, Li ZL, Du FS, Li ZC (2013) One-pot synthesis of polyamides with various functional side groups via Passerini reaction. Polym Chem 4:444–448
36. Huang QH, Yang FH, Cao XX, Hu ZY, Cheng CJ (2019) Thermally healable polyurethanes based on furfural-derived monomers via Baylis-Hillman reaction. Macromol Res 27:895–904
37. Elzubair A, Suarez JCM, Bonelli CMC, Mano EB (2003) Gel fraction measurements in gamma-irradiated ultra high molecular weight polyethylene. Polym Test 22:647–649
38. Liu Y, Wu DM, Chen WH, Ding YM, Xu H (2004) Crystallization behaviors and the mechanical properties of the chemical crosslinked ultra-high molecular weight polyethylene. Plastics 33:1–5
39. Brunelli F, Aprile S, Russo C, Giustiniano M, Tron GC (2022) In-water synthesis of isocyanides under micellar conditions. Green Chem 24:7022–7028
40. Yang T, Li WZ, Ogunbiyi AT, An SX (2021) Efficient catalytic conversion of corn stover to furfural and 5-hydromethylfurfural using glucosamine hydrochloride derived carbon solid acid in Y-valerolactone. Ind Crop Prod 161:113173
41. Tu R, Sun Y, Wu YJ, Fan XD, Cheng SC, Jiang EC, Xu XW (2021) Selective production of furfural and phenols from rice husk: the influence of synergetic pretreatments with different order. Renew Energ 168:297–308
42. Beerthuis R, Rothenberg G, Shiju NR (2015) Catalytic routes towards acrylic acid, adipic acid and ε-caprolactam starting from biorenewables. Green Chem 17:1341–1361
43. Deng WP, Yan LF, Wang BJ, Zhang QH, Song HY, Wang SS, Zhang QH, Wang Y (2021) Efficient catalysts for the green synthesis of adipic acid from biomass. Angew Chem Int Ed 60:4712–4719
44. Tran AV, Park SK, Lee HJ, Kim TY, Kim Y, Suh YW, Lee KY, Kim YJ, Baek J (2022) Efficient production of adipic acid by a two-step catalytic reaction of biomass-derived 2,5-furandicarboxylic acid. Chemsuschem 15:e202200375
45. Xu XW, Wu JH, Li MZ, Wang S, Feng HZ, Wang BB, Hu KZ, Zhang CZ, Zhu J, Ma SQ (2023) Synergistic catalytic effect of triple dynamic bonds for fast-reprocessing and high-performance cross-linked polymers. Polym Chem 14:523–532
46. Lee JM, Noh GY, Kim BG, Yoo Y, Choi WJ, Kim DG, Yoon HG, Kim YS (2019) Synthesis of poly(phenylene polysulfide) networks from elemental sulfur and *p*-diiodobenzene for stretchable, healable, and reprocessable infrared optical applications. ACS Macro Lett 8:912–916
47. Zheng T, Zhou Q, Yang T, Zhao Y, Fan B, Bo J, Fan LS, Peng RF (2022) Disulfide bond containing self-healing fullerene derivatized polyurethane as additive for achieving efficient and stable perovskite solar cells. Carbon 196:213–219
48. Luo QF, Shi CY, Wang ZX, Chen M, Qu DH (2022) Introducing the latest self-healing polymer based on thioctic acid into the undergraduate chemistry laboratory. J Chem Educ 99:3488–3496
49. Sridhar LM, Oster MO, Herr DE, Gregg JBD, Wilson JA, Slark AT (2020) Re-usable thermally reversible crosslinked adhesives from robust polyester and poly(ester urethane) Diels-Alder networks. Green Chem 22:8669–8679
50. Yang KJ, Grant JC, Lamey P, Joshi-Imre A, Lund BR, Smaldone RA, Voit W (2017) Diels-Alder reversible thermoset 3D printing: isotropic thermoset polymers via fused filament fabrication. Adv Funct Mater 27:1700318
51. Wang ZY, Zhou JP, Liang HB, Ye SQ, Zou JH, Yang HT (2020) A novel polyurethane elastomer with super mechanical strength and excellent self-healing performance of wide scratches. Prog Org Coat 149:105943